Design of a scanning Josephson junction microscope for submicron-resolution magnetic imaging

B. L. T. Plourde and D. J. Van Harlingen[a)]
Department of Physics, Science and Technology Center for Superconductivity, and Materials Research Laboratory, University of Illinois at Urbana-Champaign, Urbana, Illinois 61801

(Received 11 June 1998; accepted for publication 22 July 1999)

We describe a magnetic field scanning instrument designed to extend the spatial resolution of scanning superconducting quantum interference device microscopy into the submicron regime. This instrument, the scanning Josephson junction microscope, scans a single Josephson junction across the surface of a sample, detecting the local magnetic field by the modulation of the junction critical current. By using a submicron junction and a scanning tunneling microscope feedback system to maintain close proximity to the surface, magnetic field sensitivity of 10 μG with a spatial resolution of 0.3 μm should be attainable, opening up new opportunities for imaging vortex configurations and core structure in superconductors and magnetic domains in magnetic materials. © *1999 American Institute of Physics.* [S0034-6748(99)00311-1]

There has been much recent interest in developing magnetic imaging techniques with the smallest possible spatial resolution and highest field sensitivity. The primary motivation has been the desire to understand the dynamics and interactions of vortices in the high-temperature superconductors, but imaging capabilities also find application in the study of mesoscopic devices and magnetic materials, and for nondestructive testing. Popular imaging techniques capable of single vortex detection include scanning Hall probe microscopy (SHM),[1] in which a microfabricated Hall bar is scanned across the sample to measure the field-dependent Hall voltage, magnetic force microscopy (MFM),[2] which monitors the deflection of a small mechanical cantilever by the local magnetic field, Lorentz microscopy,[3] an electron holography technique that senses the phase shift from the magnetic fields near the vortex, and scanning superconducting quantum interference device (SQUID) microscopy (SSM),[4–6] in which a dc SQUID (or a superconducting pickup coil coupled to it) is scanned across the sample surface to measure the local fields. Each of these approaches has unique capabilities that make it advantageous in different experimental situations.

In this article, we describe a new instrument, the scanning Josephson junction microscope (SJJM), which enhances the spatial resolution of SSM by employing a single submicron Josephson junction as the magnetic sensor. This instrument should surpass all other currently available techniques in terms of magnetic flux sensitivity at the submicron scale. In addition, the positioning scheme proposed can yield information about the surface structure and chemistry that can be correlated with the magnetic field distribution. We are currently in the process of constructing such an instrument; here, we discuss the requirements and projected performance specifications of the SJJM.

The basic idea of the scanning Josephson junction microscope is shown in Fig. 1. The detector junction has a cross-strip geometry with the plane of the junction oriented perpendicular to the sample surface. The junction is situated near the end of a microfabricated scanning tunneling microscope (STM) tip. The junction/tip assembly is fixed and is cooled by thermal contact to a liquid helium cold stage. The sample is raster-scanned beneath the detector using a piezoelectric scan tube and is maintained in close proximity to the junction with a standard STM feedback control system. The local vertical magnetic field threads the junction barrier, modulating the Josephson critical current. In contrast to a dc SQUID, which exhibits a periodic modulation of the critical current with applied flux, analogous to two-slit optical interference, the critical current of a single Josephson junction displays a Fraunhofer single-slit diffraction pattern, as shown in Fig. 2. As with the dc SQUID, the flux is most easily detected by resistively shunting the junction to remove the hysteresis, then current biasing the device into the finite voltage state and monitoring the output voltage. For small signal operation, a dc magnetic flux is coupled into the junction by applying current through the upper electrode to flux bias the junction on the sharpest rise of the central diffraction peak, optimizing the flux sensitivity. Alternately, the junction can be biased at zero dc flux and an ac modulation flux can be applied. By detecting the modulated output voltage and feeding the dc level back to the flux input, the junction can be operated in a flux-locked loop that linearizes the output voltage and extends the dynamic range, as is commonly done for a dc SQUID.

The primary advantage of the SJJM is its enhanced spatial resolution. The effective flux detection area is defined by the width of the junction in one direction, and the sum of the penetration depths into the base and counterelectrode films in the other; the thickness of the tunneling barrier itself is negligible. For a microfabricated Nb technology, widths less than 1 μm can be obtained by electron-beam lithography, and the penetration depth of Nb is 39 nm, giving an effective

a)Electronic mail: dvh@uiuc.edu

 © 1999 American Institute of Physics

Downloaded 05 Dec 2001 to 130.126.102.77. Redistribution subject to AIP license or copyright, see http://ojps.aip.org/rsio/rsicr.jsp

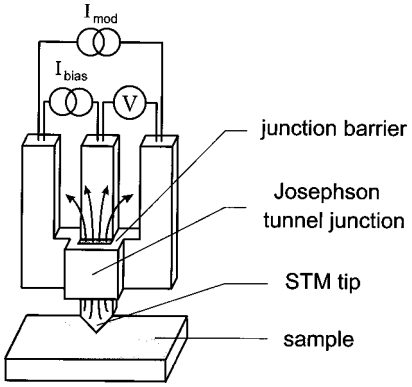

FIG. 1. Schematic diagram of the scanning Josephson junction microscope.

pickup area less than 0.1 μm^2. This is several orders of magnitude smaller than conventional scanning SQUID microscopes, which typically use pickup coils with 5–10 μm diameter. To achieve this potential spatial resolution, it is necessary to maintain the junction in close proximity to the sample surface, typically to within the detector width. To accomplish this, we fabricate the junction near the edge of a thin film conductor that serves as an STM tip. The device is then operated in a standard constant-current STM mode, which maintains the detector tip at a constant height above the surface (assuming a uniform conducting surface) as the sample is scanned. This technique was previously used to maintain the spacing of Hall probes above a sample surface.[1] A valuable by-product of this scheme is that information about the surface topography can be simultaneously obtained from the STM feedback signal. This will enable us to correlate the measured flux signal with surface features such as step edges and defects that serve as flux pinning sites.

In Fig. 2, we show the critical current of a single Josephson tunnel junction versus applied magnetic flux through the junction, which follows the characteristic Fraunhofer dependence $I_c(\Phi)=I_0|\sin(\pi\Phi/\Phi_0)/(\pi\Phi/\Phi_0)|$, provided that magnetic self-field effects from the tunneling currents can be neglected. This requires that the junction be in the small junction limit in which the Josephson penetration length $\lambda_J=(\Phi_0/2\pi\mu_0\delta J_c)^{1/2}\gg w$, the width of the junction, where J_c is the Josephson critical current density and $\delta=t+2\lambda$ is the effective magnetic thickness of the barrier that depends on the tunneling barrier thickness t and the penetration depth λ of the superconducting electrodes. Also shown in Fig. 2 is the voltage across the junction versus flux at a bias current

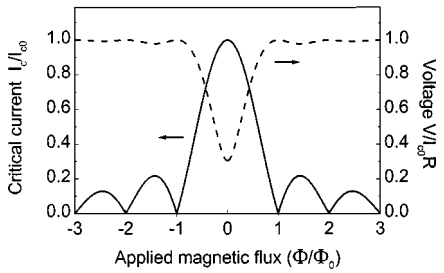

FIG. 2. Calculated critical current I_c vs applied magnetic flux Φ for a single Josephson tunnel junction. Also shown is the voltage V across the junction at a bias current of $1.05\,I_{c0}$.

just above I_c, assuming a resistively shunted junction (RSJ) for which $V=R(I^2-I_c^2)^{1/2}$. The key signal parameter is the transfer function $dV/d\Phi$ that characterizes the flux sensitivity of the junction; for the bias current shown ($I\approx 1.05\,I_0$), the maximum transfer function is approximately I_cR/Φ_0 at a flux bias of about $0.3\Phi_0$. When we add a shunt resistance R such that the junction damping parameter $\beta_c=2\pi I_cR^2C/\Phi_0<1$ to remove hysteresis in the current–voltage characteristic, then the transfer function will be have a maximum value of $dV/d\Phi=(J_c/2\pi c\Phi_0)^{1/2}$, where c is the specific capacitance of the junction. For a standard Nb trilayer technology, $J_c\approx 10^4$ A/cm^2 and $c\approx 50$ fF/μm^2, so the transfer function can be of order 1 mV/Φ_0.

The flux sensitivity of the SJJM is limited by thermal noise generated in the shunt resistance. To estimate the noise level of the single junction detector, we treat the junction as a dc SQUID with junction capacitances C_J equal to 1/2 of the single junction capacitance, and an inductance corresponding to the stripline inductance connecting the two sides of the junction. For a junction with a tunneling area of width w and length l, $C_J\approx cwl/2$ and $L\approx\mu_0\delta w/2l$. Using the standard expression for the energy resolution of an optimized, thermally limited dc SQUID,[7] $S_E\approx 16k_BT(\mathrm{LC})^{1/2}=8k_BTw(\mu_0\delta c)^{1/2}$. For a junction of width 1 μm, operated at 4.2 K, this thermal limit expression yields a flux resolution of $S_\Phi\approx 10^{-9}\,\Phi_0/\mathrm{Hz}^{1/2}$ and a corresponding energy resolution of $S_E\approx 0.05\,\hbar$, well below the predicted quantum limit $S_E\approx\hbar$ for a dc SQUID.[8] Thus, in principle the single junction detector is capable of achieving quantum-limited performance as a result of its low intrinsic inductance and direct flux pickup. However, since the required optimization conditions,[7] $\beta_c=2\pi I_cR^2C/\Phi_0=1$ and $\beta=2LI_c/\Phi_0=1$, would require an unreasonably large current density in the junction, the sensor will in practice be operated in the low-β regime,[7] for which $S_E\sim\beta^{-3/2}$. For a typical current density of 10^4 A/cm^2, this yields a more realistic but still impressive flux resolution of order $5\times 10^{-8}\,\Phi_0/\mathrm{Hz}^{1/2}$. For comparison, the best performance recorded for a comparably sized Hall bar is of order $10^{-5}\,\Phi_0/\mathrm{Hz}^{1/2}$.[9]

We have studied the imaging potential of the SJJM by simulating the modulation of the junction critical current for different junction parameters and magnetic field distributions. We assume that the magnetic field threading the junction is confined to the plane of the junction (B_x,B_z) because the component along the tunneling direction (B_y) is screened by the superconducting electrodes. The net critical current is found by integrating the local supercurrent density over the junction area

$$I_c=\max\left\{\int_{-w/2}^{w/2}dx\int_0^l dz J_c(x,z)\sin\phi(x,z,\phi_0)\right\}, \qquad (1)$$

where $\phi(x,z,\phi_0)$ is the gauge-invariant phase difference across the junction relative to the phase drop ϕ_0 at the center of the bottom edge of the junction ($x=0$, $z=0$). The maximum is found by varying ϕ_0. In the short junction limit, the phase difference depends on the magnetic field distribution in the junction according to

Downloaded 05 Dec 2001 to 130.126.102.77. Redistribution subject to AIP license or copyright, see http://ojps.aip.org/rsio/rsicr.jsp

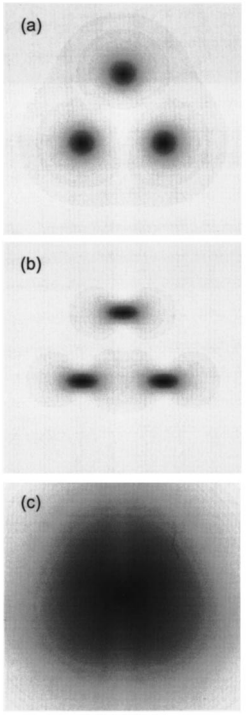

FIG. 3. Images of three vortices with separation 3.46 μm, corresponding to a magnetic field of 2 G. The scan area is 10 μm$\times$10 μm. (a) Calculated vertical component of the magnetic field B_z, (b) simulated SJJM image for a 1 μm$\times$1 μm junction scanned at a height of 0.2 μm, and (c) simulated SSM image for a 5-μm-diam SQUID loop scanned at a height of 2 μm.

$$\phi(x,z,\phi_0)=\left[\frac{2\pi\delta}{\Phi_0}\left(\int_0^z dz' B_x(0,z') - \int_0^x dx' B_z(x',z)\right)+\phi_0\right]. \quad (2)$$

The scanning process can be simulated by generating the vector magnetic field from a given distribution of sample currents and/or magnetic moments, then stepping the junction across it at a fixed height above the surface. The perturbation of the ambient magnetic field from Meissner screening by the superconducting electrodes and the subsequent focusing of flux through the junction is difficult to calculate exactly. As an approximation, we assume that B_x, the horizontal field parallel to the junction, is unchanged, whereas B_y, the horizontal field in the tunneling direction, is screened to zero; the vertical field B_z is taken to be uniform, equal to its value at the bottom edge of the junction. By including realistic parameters for the junction, we can calculate the magnetic feedback flux applied to the junction in a flux-locked mode, the actual experimentally measured quantity.

Vortices in superconductors provide a useful field distribution to test the performance of the SJJM because they diverge significantly above the surface of the superconductor. Near the surface of a thin superconducting film, a vortex can be modeled as a magnetic monopole situated one effective thin film penetration length below the surface.[10] Figure 3 shows the signal output for a junction of area 1 μm$\times$1 μm scanned at height 0.2 μm from the bottom of

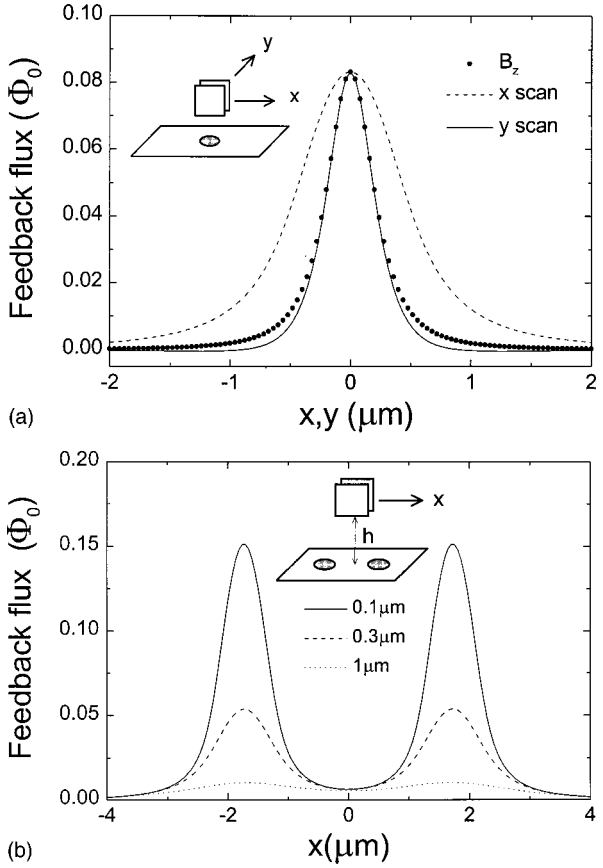

FIG. 4. (a) Predicted spatial variation of the magnetic flux detected by the SJJM from a single vortex scanned at a height of 0.2 μm in the x (parallel to the junction) and y (perpendicular to the junction) directions. For comparison, the points show the vertical component of the magnetic field at the center of the lower edge of the junction, normalized to the peak flux value. (b) Predicted dependence of the SJJM flux on the separation of the lower edge of the detector junction and the sample surface for a scan over two adjacent vortices separated by 3.46 μm.

the junction over three neighboring vortices spaced 3.46 μm apart, corresponding to a magnetic field of 2 G. For comparison, we also show the distribution of the local vertical magnetic field from these vortices, and the image that would be obtained for this distribution with a scanning SQUID microscope with a 5-μm-diam pickup coil. In contrast to the SSM image, the SJJM easily resolves the vortices, but the image also reflects the asymmetry of the detector junction. This is

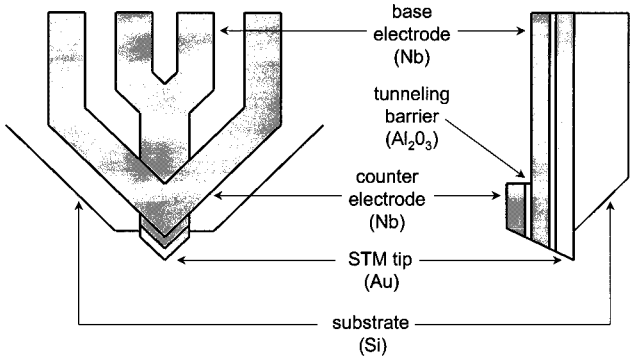

FIG. 5. Proposed design for the SJJM detector, showing the integrated Josephson tunnel junction and STM tip extending off the edge of an etched Si substrate.

Downloaded 05 Dec 2001 to 130.126.102.77. Redistribution subject to AIP license or copyright, see http://ojps.aip.org/rsio/rsicr.jsp

seen most clearly by comparing line scans across a single vortex in directions parallel and perpendicular to the junction tunneling direction, as shown in Fig. 4(a).

The most critical requirement for obtaining high-spatial resolution images is the ability to maintain the lower edge of the detector junction near the sample surface during the scan. The strong sensitivity of the image to the sample-detector distance is demonstrated in Fig. 4(b), which shows SJJM voltage signal obtained for a line scan at different heights over two adjacent vortices. As expected, both the magnitude of the detected flux and the spatial resolution drop precipitously when the detector distance is larger than its spatial dimensions. To achieve close proximity of the detector, we have developed the detector design shown in plan and edge views in Fig. 5; we are in the process of implementing this design. In this scheme, the junction is a cross-strip geometry fabricated on top of an electrically isolated thin film STM tip. The junction-tip assembly extends over the edge of the Si wafer. This is achieved by fabricating the structure over a SiN window formed by anisotropic etching of the Si substrate from the backside. The bottom edge of the junction and the STM tip are simultaneously defined by ion milling at an angle, ensuring a tip/junction separation less than 0.1 μm. The SiN membrane is subsequently removed by reactive-ion etching. This design also highlights what we consider to be one of the most serious concerns about the SJJM—the magnetic field generated by the flux bias current. For a junction of dimensions $l \times w$ and magnetic thickness δ, the mutual inductance of the flux bias line to the junction is $M = \mu_0 \delta l/w$. Thus, for a junction area of $1\,\mu\text{m} \times 1\,\mu\text{m}$, a flux bias at the maximum transfer function point ($\Phi \approx 0.3\,\Phi_0$) would require a current of about 5 mA. If unscreened, this current would generate a substantial magnetic field ($\sim$10 G) at the sample surface. In practice, this field will be greatly reduced [$\sim(\delta/l)^2 \approx 0.01$] by the screening of the superconducting base electrode that ground planes the flux bias line, but the fringing field may still be a concern for some low field applications.

It is interesting to consider the ultimate limit of the SJJM. With electron-beam lithography, it should be possible to reduce the junction dimensions to about 0.1 μm, giving a flux pickup area of only $10^{-2}\,\mu\text{m}^2$, nearly four orders of magnitude smaller than our present SSM pickup loop. This is comparable to the smallest Hall probes that can be fabricated. With this size and an expected (optimized) flux sensitivity of $10^{-8}\,\Phi_0$, the projected field sensitivity is of order 10 μG, substantially better than the maximum sensitivity of the Hall probe. However, for some measurements this advantage in sensitivity is offset by the advantages Hall probes offer in terms of temperature and magnetic field range. In both cases, it is necessary to maintain a close sample-detector spacing to achieve the ultimate spatial resolution.

This is work supported by the NSF Science and Technology Center for Superconductivity under Grant No. NSF DMR91-20000, and by the Department of Energy through Grant No. DEFG02-96ER-45439. We also acknowledge use of the microfabrication and computer facilities of the Frederick Seitz Materials Research Laboratory at the University of Illinois.

[1] A. M. Chang, H. D. Hallen, L. Harriot, H. F. Hess, H. L. Kao, J. Kwo, R. E. Miller, R. Wolfe, J. van der Ziel, and T. Y. Chang, Appl. Phys. Lett. **61**, 1974 (1992).
[2] Y. Martin, D. Rugar, and H. K. Wickramasinghe, Appl. Phys. Lett. **52**, 244 (1988).
[3] K. Harada, T. Matsuda, J. Bonevich, M. Igarashi, S. Kondo, G. Pozzi, U. Kawabe, G. Pozzi, U. Kawabe, and A. Tonomura, Nature (London) **360**, 51 (1992).
[4] L. N. Vu and D. J. Van Harlingen, IEEE Trans. Appl. Supercond. **3**, 1918 (1993); L. N. Vu, M. S. Wistrom, and D. J. Van Harlingen, Appl. Phys. Lett. **63**, 1693 (1993).
[5] A. Mathai, D. Song, Y. Gim, and F. C. Wellstood, Appl. Phys. Lett. **61**, 598 (1992).
[6] J. R. Kirtley, M. B. Ketchen, K. G. Stawiasz, J. Z. Sun, W. J. Gallagher, S. H. Blanton, and S. J. Wind, Appl. Phys. Lett. **66**, 1138 (1995); J. R. Kirtley, M. B. Ketchen, C. C. Tsuei, J. Z. Sun, W. J. Gallagher, L.-S. Yu-Jannes, A. Gupta, K. G. Stawiasz, and S. J. Wind, IBM J. Res. Dev. **39**, 655 (1995).
[7] C. D. Tesche and J. Clarke, J. Low Temp. Phys. **27**, 301 (1977).
[8] R. H. Koch, D. J. Van Harlingen, and J. Clarke, Phys. Rev. Lett. **45**, 2132 (1980).
[9] A. Oral, S. J. Bending, and M. Henini, Appl. Phys. Lett. **69**, 1324 (1996).
[10] J. Pearl, Appl. Phys. Lett. **5**, 65 (1964).

Downloaded 05 Dec 2001 to 130.126.102.77. Redistribution subject to AIP license or copyright, see http://ojps.aip.org/rsio/rsicr.jsp